# Tunable Self-Assembly of Cellulose Nanowhiskers and Polyvinyl Alcohol Chains Induced by Surface Tension Torque

**ARTICLE** *in* BIOMACROMOLECULES · NOVEMBER 2013

Impact Factor: 5.75 · DOI: 10.1021/bm401287s · Source: PubMed



**5 AUTHORS**, INCLUDING:

Mahdi Mashkour
Gorgan University of Agricultural Sciences and…
**9** PUBLICATIONS **25** CITATIONS
SEE PROFILE

Fumiko Kimura
Kyoto University
**60** PUBLICATIONS **709** CITATIONS
SEE PROFILE

Mehrdad Mashkour
Babol Noshirvani University of Technology
**3** PUBLICATIONS **4** CITATIONS
SEE PROFILE

Article

pubs.acs.org/Biomac

# Tunable Self-Assembly of Cellulose Nanowhiskers and Polyvinyl Alcohol Chains Induced by Surface Tension Torque

Mahdi Mashkour,*[,†,‡] Tsunehisa Kimura,[‡] Fumiko Kimura,[‡] Mehrdad Mashkour,[§] and Mehdi Tajvidi[∥]

[†]Department of Wood Engineering and Technology, Faculty of Wood and Paper Engineering, Gorgan University of Agricultural Sciences and Natural Resources, Gorgan 49189-43464, Iran

[‡]Fibrous Biomaterials Laboratory, Division of Forest and Biomaterials Science, Graduate School of Agriculture, Kyoto University, Kyoto 606-8502, Japan

[§]Department of Biotechnology, Faculty of Chemical Engineering, Babol Noshirvani University of Technology, Babol 47148-71167, Iran

[∥]School of Forest Resources, University of Maine, Orono, Maine 04469, United States

**ABSTRACT:** This article focuses on the formation of the surface tension torque (STT) phenomenon close to the dry-line boundary layer during evaporation of the liquid phase of a solution casted shape-anisotropic nanoparticle suspension (here, cellulose nanowhisker (CNW)) or dissolved polymer (here, polyvinyl alcohol (PVA)) and its effects on self-assembly of the cellulose nanocrystals and polymer chains. The results confirm that the STT tends to align both the CNWs and the PVA chains tangential to the dry-line boundary layer. By careful control of the advancement of the dry-line, achieving special linear and curved patterns of both the CNWs and the PVA chains proportional to the mold position and geometry is possible. The STT phenomenon is explained and simplified in terms of a physical model. Understanding of the STT phenomenon and its effects on the alignment and self-assembly of the CNWs and PVA chains is necessary especially when achieving alignment using a modulated external magnetic or electric field is desired. The STT is safe, inexpensive, easy, and efficient, and can be a good alternative to the magnetic and electric field orientation methods.

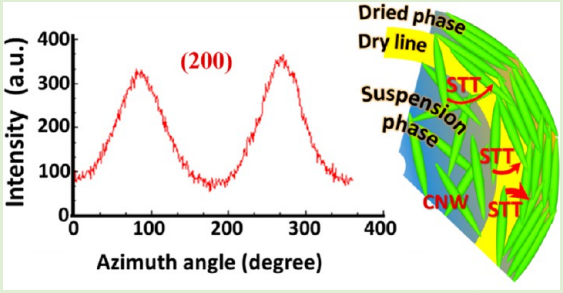


## INTRODUCTION

Aligning and patterning of nanoparticles with the aim of obtaining unique properties is one of the most interesting research topics in the field of designing and creating advanced materials.[1−6] Rod-like cellulose nanowhiskers (CNWs) are known as one of the most promising potential nanobiomaterials with some unique characteristics that comply with the needs of advanced materials.[7,8] Low density, high specific mechanical properties, small thermal expansion coefficient, high surface to volume ratio, high surface reactivity and ability to functionalize, and piezoelectric properties are among the most promising engineering characteristics of the CNWs.[7−10] Because cellulose chains are inherently arranged along the long axis, the CNWs are physically and mechanically anisotropic, thereby making CNW alignment control a critical key to achieving the highest levels of material properties, especially while fabricating an advanced material.[10−13]

Here, we proved that surface tension torque (STT) can be effectively used to control the alignment of CNWs and to fabricate thin films and nanocomposites with desired micro- and nanopatterns. The STT refers to a surface tension induced rotating moment which can affect orientation of the CNWs and polymer chains in aqueous suspensions close to the dry-line boundary and align them parallel to the dry line. In the other words, the method which we report here is an STT induced self-assembly method. In summary, the physical basis of this method is based on using the combined effects of two main driving forces close to the dry-line boundary layer: surface tension gradient and surface evaporation. These driving forces act on the anisotropic cellulose nanowhiskers, and the resultant surface tension torques, which are proportional to the length of CNWs and the horizontal contact angle between the CNWs and the surface of the glass substrate, rotates the CNWs and aligns them parallel to the dry-line boundary layer. There are several reports on using surface tension torque for reconfiguring metal solder microstructures into full three-dimensional geometries, but the applied physical terms and conditions and driving forces are quite different.[14−19] Review of the literature revealed that there is no report on the self-assembly of CNWs and polymer chains induced by the STT. To date, a number of methods to align CNWs including using shear stress and strong magnetic and AC electric fields and more recently a convective-shear assembly system have been used.[10−13,20−26] Because of some inherent problems, none of these methods has been extended beyond the research laboratory scale. The large amount of time and high energy consumption, high technical

Received: August 28, 2013
Revised: November 14, 2013
Published: November 18, 2013

  

expertise requirements, the expensive proprietary technology required, and dimensional restrictions are some of the most important challenges ahead of scaling up these methods.[27,28] Furthermore, unsafe and harmful effects of human exposure to strong magnetic and electric fields are well-known.[27,29,30] The STT method seemingly has none of these problems. The STT method described here is very simple, quick, efficient, and completely safe. However, this method provides the possibility to produce some interesting curved nanopatterns resulting in careful alignment control of the CNWs at the nanoscale, a possibility not available with other methods.

## EXPERIMENTAL SECTION

**Cellulose Nanowhisker (CNW) Preparation.** Cellulose nanowhiskers were extracted from purified cellulose powder (CF-11; Whatman Co.) by acid hydrolysis in 3 N hydrobromic acid (Nacalai Tesque Inc.) for 4 h at 100 °C. To quench acid hydrolysis, dilution was performed two times, and the suspension was ultracentrifuged for 15 min at 10,000 rpm for purification. The liquid phase was removed by decantation, and the solid residue was resuspended and ultracentrifuged again under the same conditions. This step was repeated several times to obtain a turbid supernatant. The CNC suspension was poured onto a filter membrane and repeatedly dialyzed in distilled water until a relatively neutral pH was obtained.

**Preparation of Cellulose Nanowhisker−PVA Suspension.** A 10 wt % of PVA solution was made by dissolving PVA (Wako Pure Chemical Industries, Ltd.; average degree of polymerization = 1500−1800) in distillated water at 60 °C overnight while magnetically stirring, and then, the cellulose nanowhisker suspension was slowly added to the prepared PVA solution to make a 0.2 wt % suspension of cellulose nanowhiskers in the dissolved PVA. The PVA concentration of the final suspension was about 5 wt %. To homogeneously disperse cellulose nanowhiskers into the PVA solution, ultrasonic treatment was carried out for 2 min.

**Preparation of the Nanopatterned Films.** A 0.2 wt % cellulose nanowhisker suspension and a 0.2 wt % cellulose nanowhisker−PVA suspension were carefully cast into previously prepared molds and oven-dried at 80 °C. The molds were different in shape and geometry. Two were cubic with flat bottoms of which one was placed inside the oven horizontally, while the other was inclined. To make curved nanopatterned films, a watch glass with a diameter of 5 cm was used as the curved mold.

**Characterization.** The extracted CNWs were characterized using a scanning probe microscopy (SPM) system (Shimadzu SPM-9500, Shimadzu) in the atomic force microscope (AFM) mode. The alignments of the CNWs and polymer chains were studied using an Olympus ModelX2POL polarized light microscope and a Rigaku Rapid II X-ray diffraction system (Mo K-alpha radiation, 50 kV and 100 mA).

## RESULTS AND DISCUSSION

The CNWs were chemically extracted from cotton cellulose powder using acid hydrolysis. To investigate the STT efficiency at both micro- and nanoscales, a combination of CNWs and cellulose microcrystals (CMCs) was used to make films by solution casting. Figure 1a shows a field emission scanning electron micrograph of the combination of CMCs and CNWs that was used to make the final films. Figure 1b shows an atomic force micrograph of the CNWs content. The length and diameter of the CNWs were characterized as being 180 ± 10 and 6 ± 2 nm, respectively. Using a polarized light microscope (POM), the fabricated CMC−CNW films were studied (Figure 1c). Figure 1d and e was obtained by the polarized light microscopy examination of two cellulose thin films made by casting a 0.2% CNW and CMC water suspension into the same flat bottomed mold and oven-drying. As can be seen, the results

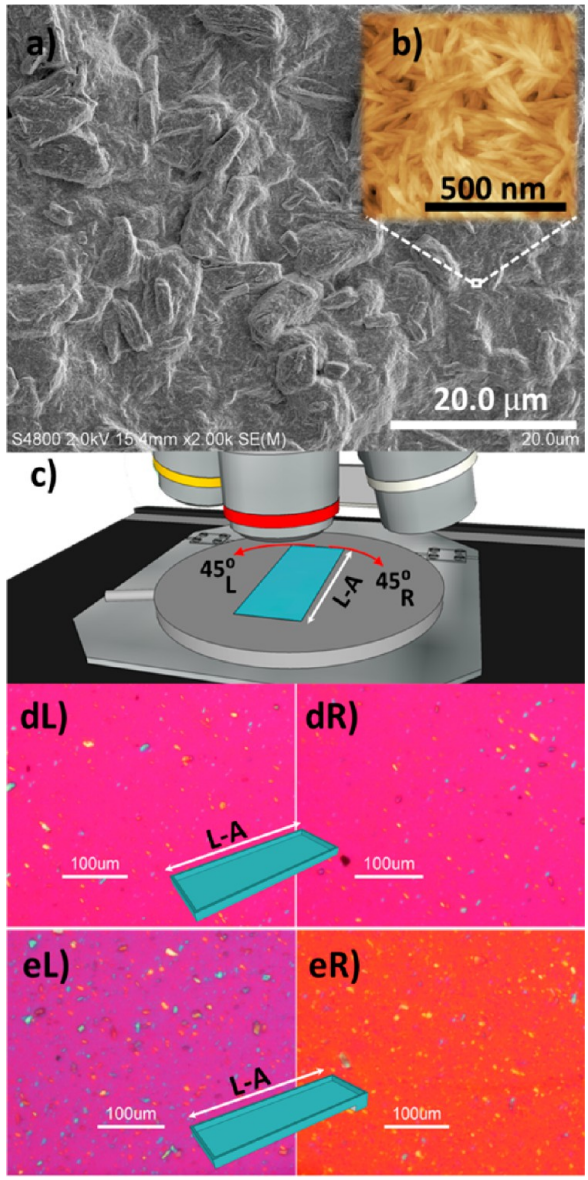


**Figure 1.** (a) FE-SEM micrograph of a combination of CMCs and CNWs, (b) AFM micrograph of the CNWs, and (c) schematic showing the position and rotation of the fabricated films when the POM study was performed (L and R indicate the 45° rotation directions of the stage to the left and right, respectively, and L-A indicates the long-axis of the fabricated film). dL and dR show the optical behavior of the film fabricated by solution casting and horizontally setting the mold. eL and eR present the optical behavior of the film fabricated by solution casting and setting the mold slightly inclined parallel to the long-axis.

are clearly different. The Figure 1d series is related to the cellulose thin film formed when the mold was horizontally placed in the oven, while the micrographs in the Figure 1e series were obtained from the film formed when the mold was slightly inclined with respect to the horizontal oven floor. In both cases, the CMCs did not align. These results strongly indicate that unlike CMCs, when the mold is placed at an incline with respect to the horizon, a strong force acts on CNWs in such a way to align them, which is in contrast to the case when the mold is horizontally placed.

To determine the orientation direction of the CNWs, a cellulose microfiber was used as the microscale model. Because


dx.doi.org/10.1021/bm401287s | Biomacromolecules 2014, 15, 60−65

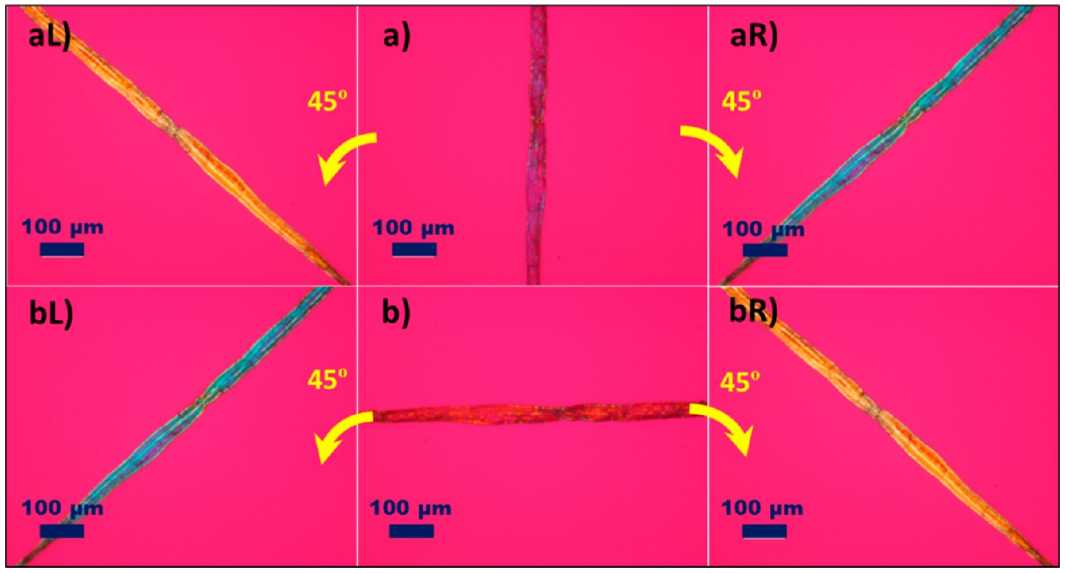


**Figure 2.** (a series) POM images of a single plant cellulose fiber and its optical response when rotated 45° from the vertical position to the left (aL) and to the right (aR). (b series) POM images of the same fiber and its optical response when rotated 45° from the horizontal position to the left (bL) and to the right (bR).

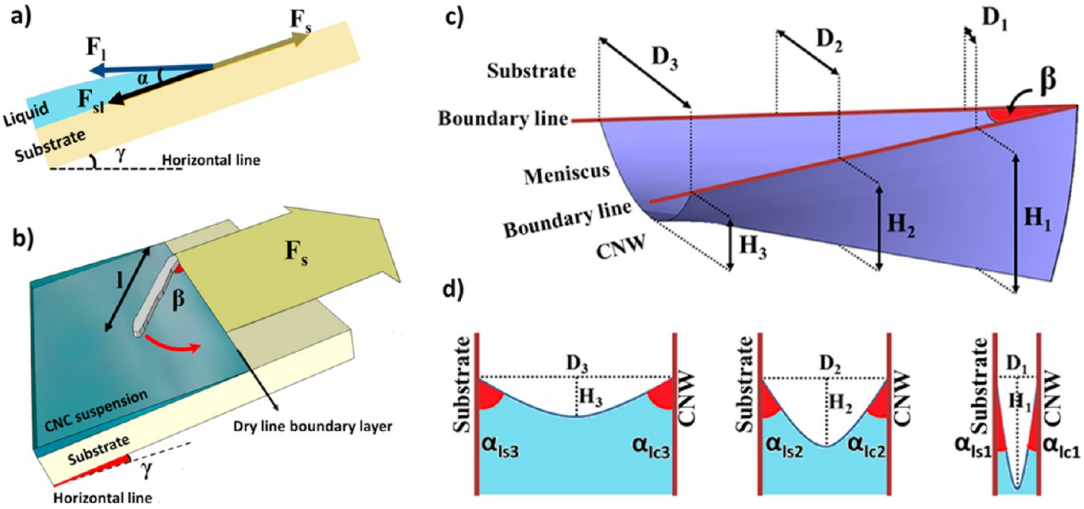


**Figure 3.** (a) Modulated forces on the dry-line boundary layer. (b) A schematic model that shows how the surface tension torque forces the CNW to align tangential to the dry boundary layer. (c) Capillary force gradient between the CNW and dry boundary line. (d) Changes of the contact angles between the liquid phase and substrate surface ($\alpha_{ls}$) and liquid phase and CNW ($\alpha_{lc}$) proportional to changes of the capillary force gradient. ($F_s$, surface tension force of the substrate; $F_l$, surface tension force of the liquid; $F_{sl}$, interfacial surface tension force; $D$, distance between the CNW and the dry-line boundary layer; $H$, maximum curvature of the liquid surface in the meniscus region; $\alpha_{ls}$, contact angle between the liquid phase and substrate; and $\alpha_{lc}$, contact angle between the liquid phase and CNW.)

of the same orientation direction of cellulose chains in cellulose nanowhiskers and microfibers, i.e., the chains aligned parallel to the long axis, their response to the polarized light should be the same. Examination of the microfiber model using a polarized light microscope and observation of its color changes with rotation have shown that the CNWs were unidirectionally aligned perpendicular to the direction of the incline. Figure 2 series show the color changes of the cellulose microfiber model under a polarized light microscope.

To explain this observation, the authors suggest a mechanism based on capillary force gradient and STT phenomena close to the dry-line boundary layer. Most recently, a number of scientists have suggested some phenomena such as coffee-ring effect and droplet evaporation effect, which are based on the capillary forces.[31−33] The mechanism which is proposed and explained here has some similarities to the already proposed ones. The alignment probably occurs very close to the interface between the liquid phase and the inclined dry surface. Brownian motion and the surface tension are probably the most important forces that control the alignment of the CNWs. The Brownian motion induced movement of these colloidal nanoparticles allows them to rotate and translate freely, but their orientation may change when effective external modulated forces become dominant, for example, a force that is utilized better on an inclined surface compared with a flat surface. The dry-line boundary is an air/suspension/substrate triple line. The free energy of a CNW located on this triple line is different from that of a CNW located in a suspension phase. It may be


dx.doi.org/10.1021/bm401287s | Biomacromolecules 2014, 15, 60−65

lower or higher, depending on the interaction of the CNW with the suspending medium, substrate, and air. In addition, if a CNW is located on the triple line, the area of suspending liquid exposed to the air is reduced, resulting in the reduction of the surface free energy of the suspending liquid. This favors the CNW to be located on the triple line. Let us assume that the contact of a CNW with the triple line is energetically favorable. Consider that a CNW in the suspension happens to approach the triple line by Brownian motion of water molecules and/or convection flow until one of its ends contacts the triple line. The CNW may stay at this contact point, but since the contact line is energetically more favorable, a torque (we refer to this torque as surface tension torque, STT) acts, rotating the CNW toward the contact line. Once this happens, other CNWs supplied from the suspension can accumulate onto the CNWs already located on the triple line upon evaporation of the suspending liquid. Close to the dry boundary layer, the surface tension is dominant and strongly affects the colloidal nanoparticles as the most effective externally applied force. The torque due to the surface tension rotates the CNWs perpendicular to the direction of the advancing dry line and parallels them to the dry boundary layer. Figure 3 schematically shows how the CNW is affected by the torque as a result of surface tension.

Generally, the magnitude of the torque ($\tau$) is given by[34]

$$\tau = lF\sin\theta \tag{1}$$

where $l$ is the length (or magnitude) of the lever arm vector, $F$ is the magnitude of the force, and $\theta$ is the angle between the force vector and the lever arm vector. If $F$ is the surface tension force, its magnitude is given by

$$F = \sigma l \tag{2}$$

where $\sigma$ is the surface tension, and $l$ is the length on which surface tension works.

As can be seen, the CNW that is close to the dry boundary layer is affected by a surface tension torque ($\tau_s$) that is a function of the two angles designated as $\alpha$ and $\beta$ in Figure 3a and b, respectively. $\alpha$ is the contact angle or the angle between the surface tension force of the liquid ($F_l$) and the interfacial surface tension force ($F_{sl}$), which is defined as the same contracting force between two immiscible materials. $\beta$ is the angle between the long axis of the affected CNW and the dry-line boundary layer, and its magnitude is variable between a minimum ($\varepsilon$) to $\pi/2$. $F_s$ refers to the surface tension force of the substrate, and $\gamma$ is the angle of incline of the substrate relative to the horizon. Decreasing $\beta$ means tending CNW tangent to the dry-line boundary layer. The authors believe that when a CNW comes close to the dry line and the end of the CNW contacts the substrate surface, a capillary force gradient forms in the area between the substrate surface and the CNW (Figure 3c). As can be seen, the maximum capillary force is exerted close to the contact point of the CNW and substrate surfaces from where the capillary force gradually decreases to the other end of the CNW. Because CNWs are affected by the Brownian motion of water molecules, the existence of this gradient leads to turning CNWs parallel to the dry line to minimize the capillary gradient. In fact, decreasing $\beta$ angle means decreasing capillary gradient to the direction of increasing capillary forces. However, with decreasing $\beta$ angle and capillary gradient, the $\alpha_{ls}$ and $\alpha_{lc}$ decrease as well (Figure 3d). $\alpha_{ls}$ and $\alpha_{lc}$ are the contact angles between liquid phase and substrate surface, and liquid phase and CNW, respectively. Because of the different surface energies of the substrate surface and the CNW surface, these two contact angles are probably different and are therefore designated different subscripts. The decreasing $\beta$ angle is equal to enlarging the effective surface tension force, which acts on the CNW and tends to pull it on the substrate surface and align it parallel to the dry-line direction. The effects of decreasing the $\beta$ and $\alpha$ angles on the magnitude of the effective surface tension force are given by eqs 3 and 4:

$$F_s = F_{sl} + F_l \sin(\pi/2 - \alpha) \tag{3}$$

Therefore, according to eq 1, the surface tension torque ($\tau_s$) that affects the CNW and aligns it is given by eq 4:

$$\tau_s = lF_s \sin(\pi/2 - \beta) \tag{4}$$

where $l$ is the length of the CNW meaning that longer CNWs are subject to the higher STT.

STT is a potentially powerful method that makes possible good alignment control of colloidal nanoparticles such as the CNWs. The results presented hereafter will prove that the efficiency of this technique for aligning polymer chains when the liquid phase of the polymer solution (here PVA) should evaporate to form the final film is also excellent. The mechanism of aligning the PVA chains tangential to the dry boundary layer and parallel to the alignment direction of the CNWs seems to be due to the same effect of the STT. After the dissolution of PVA in the solvent (distillated water, here), individually dispersed polymer chains will be subject to the Brownian motion of water molecules, and once close to the dry boundary layer, the STT acts and affects their orientation in the same manner as that for the CNWs.

Figure 4a to f shows polarized light microscope images that indicate the successful fabrication of a curved nanopattrened CNW film, pure polyvinyl alcohol (PVA) film, and CNW-PVA nanocomposite film by controlling the alignment of CNWs and polymer chains at the nanoscale. All films were fabricated by solution casting into a concave glass mold. As can be seen, all produced films represented good alignment of both CNWs and polymer chains at nanoscale, and yet a centric circular nanopattern proportional to the geometry of the concave mold was also obtained.

Figure 5 shows AFM micrographs obtained from the surface of the CNW film fabricated by solution casting into the concave glass mold and removing the liquid phase by evaporation. As can clearly be seen, a little far from the center, the CNWs were well aligned (Figure 5a), but at the center, alignment was not good (Figure 5b). It seems that the STT effect to align CNWs decreases at the center resulting from continuous reduction of the angle incline of the concave mold and gradual transition from the inclined to flat surface. However, close to the center, some interference in self-assembly of the CNWs due to forces being applied from other directions may occur, which disrupts the centric circular pattern.

Figure 6a shows a photo of the final fabricated transparent curved patterned CNW-PVA nanocomposite, and Figure 6b displays an observation of this film between crossed polarized films. This Figure indicates the formation a "Maltese cross" pattern similar to the pattern which can be seen after the crystallization and growth of spherulite structures in polymers. Despite the apparent similarity, the formation mechanism of "Maltese cross" patterns resulting from the progression of crystallization and growth of the spherulites is not same as what happens here. Formation of the spherulite crystal starts by


dx.doi.org/10.1021/bm401287s | Biomacromolecules 2014, 15, 60−65

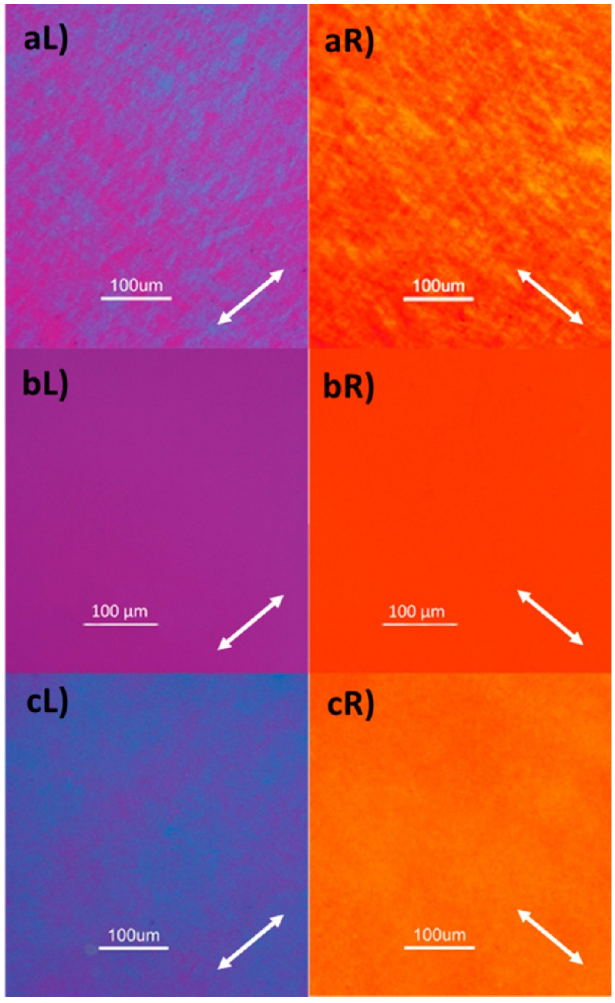


**Figure 4.** Polarized microscope observations of the unidirectionally aligned CNW film (aL and aR), pure PVA film (bL and bR), and CNW-PVA nanocomposite film (cL and cR). The arrows indicate the alignment direction.

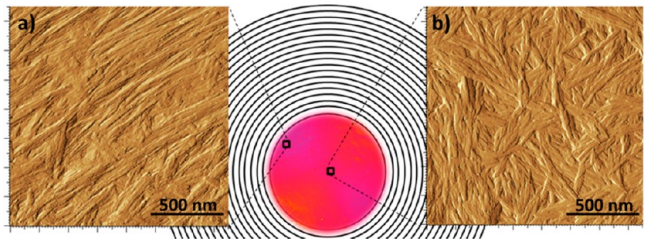


**Figure 5.** AFM micrographs from the surface of CNW film made by a drying solution casted suspension into a concave glass mold: two scanning areas of 1.5 $\mu$m × 1.5 $\mu$m (a) far from center and (b) at the center.

nucleation, and its growth is radially from center to the outside,[33] while here, the solidification and formation of the film develop from the outside to the center along with the progress of evaporation and lack of nucleation. Distribution quality of the bright and dark regions proved the formation of the centric circular pattern. Nishida and Takahashi reported the observation of such a centric circular pattern during the drying process of a methylcellulose aqueous solution.[33] The centric circular lines schematically show the centric circular alignment of the CNWs and the PVA chains in the structure of the final

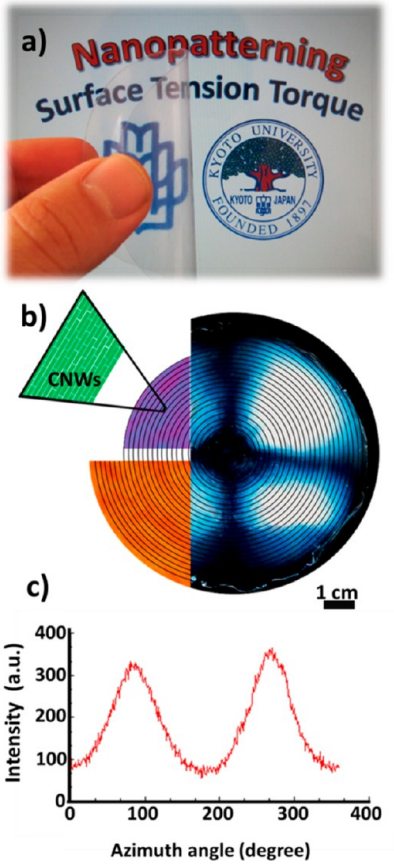


**Figure 6.** (a) Photograph of the final transparent centric circular nanopatterned CNW-PVA nanocomposite film. The Kyoto University logo is used with permisson from Kyoto University. (b) Observation of curved nanopatterned CNW-PVA nanocomposite films between crossed polarized films. (c) Relative integrated intensity distribution along the Debye ring of the (200) CNW reflections, as a function of the azimuthal angle.

CNW−PVA nanocomposite film. X-ray diffraction examination proved that the alignment of the CNWs inside the PVA matrix was excellent, even close to the center of the film (Figure 6c). However, due to the above mentioned reasons, very close to the center area, alignment quality was not good.

Note that the STT effect on the quality of alignment of the CNWs and PVA chains is not always desired. The authors believe that the STT is one of the most important reasons that negatively affect magnetic and electrical alignment when a liquid suspension evaporates to form the final film. The strong magnetic or electric field forces the CNWs and PVA chains to align perpendicular and parallel to the field direction, respectively, whereas the STT acts as a strong disruptive force and destroys the alignment. Therefore, a considerable amount of energy is needed to overcome the STT and align CNWs magnetically or electrically, and the final alignment is often not satisfactory. Understanding the STT phenomenon may help overcome some difficulties currently present during alignment processes.

## CONCLUSIONS

In summary, we demonstrated here that the STT can be used to control the alignment of CNWs and soluble polymer chains. The efficiency of the alignment is superior to the previously reported methods. In addition to the efficient control of


dx.doi.org/10.1021/bm401287s | Biomacromolecules 2014, 15, 60−65

unidirectional alignment of the CNWs and polymer chains, the STT method can be used to create new curved nano- and micropatterns, an advantage not available from any previously introduced method. The STT method is executable with no need for long time and high energy consumption, high technical expertise, and expensive proprietary technology.

## AUTHOR INFORMATION


### Corresponding Author

*Phone: +98-171-442-7050. Fax: +98-171-442-7176. E-mail: mashkour@gau.ac.ir.


### Notes

The authors declare no competing financial interest.

## ACKNOWLEDGMENTS

This work was supported by the Graduate School of Agriculture, Kyoto University and the International Scientific Cooperation office, Gorgan University of Agricultural Sciences and Natural Resources through a Collaborative Research Program.

## REFERENCES


(1) Liu, Z.; Jiao, L.; Yao, Y.; Xian, X.; Zhang, J. *Adv. Mater.* **2010**, *22*, 2285−2310.
(2) Kim, M.; Kang, B.; Yang, S.; Drew, C.; Samuelson, L. A.; Kumar, J. *Adv. Mater.* **2006**, *18*, 1622−1626.
(3) Liu, S.; Zhou, J.; Zhang, L.; Guan, J.; Wang, J. *Macromol. Rapid Commun.* **2006**, *27*, 2084−2089.
(4) Piao, G.; Kimura, F.; Takahashi, T.; Moritani, Y.; Awano, H.; Nimori, S.; Tsuda, K.; Yonetake, K.; Kimura, T. *Polym. J.* **2007**, *39*, 589−592.
(5) Kim, J. H.; Jung, Y.; Chung, J. W.; An, B. K.; Park, S. Y. *Small* **2009**, *5*, 804−807.
(6) Shastry, T. A.; Seo, J. W. T.; Lopez, J. J.; Arnold, H. N.; Kelter, J. Z.; Sangwan, V. K.; Lauhon, L. J.; Marks, T. J.; Hersam, M. C. *Small* **2012**, *9*, 45−51.
(7) Samir, M. A. S. A.; Alloin, F.; Dufresne, A. *Biomacromolecules* **2005**, *6*, 612−626.
(8) Habibi, Y.; Lucia, L. A.; Rojas, O. J. *Chem. Rev.* **2010**, *110*, 3479−3500.
(9) Eichhorn, S. J. *Soft Matter* **2011**, *7*, 303−315.
(10) Pullawan, T.; Wilkinson, A. N.; Eichhorn, S. J. *Biomacromolecules* **2012**, *13*, 2528−2536.
(11) Kimura, F.; Kimura, T. *Sci. Tech. Adv. Mater.* **2008**, *9*, 024212.
(12) Li, D.; Liu, Z.; Al-Haik, M.; Tehrani, M.; Murray, F.; Tannenbaum, R.; Garmestani, H. *Polym. Bull.* **2010**, *65*, 635−642.
(13) Sugiyama, J.; Chanzy, H.; Maret, G. *Macromolecules* **1992**, *25*, 4232−4234.
(14) Syms, R.; Yeatman, E. *Electron. Lett.* **1993**, *29*, 662−664.
(15) Syms, R. R.; Yeatman, E. M.; Bright, V. M.; Whitesides, G. M. *J. Microelectromech. Syst.* **2003**, *12*, 387−417.
(16) Syms, R. R. *J. Microelectromech. Syst.* **1995**, *4*, 177−184.
(17) Syms, R. *Electron. Lett.* **1999**, *35*, 1157−1158.
(18) Syms, R. *Electron. Lett.* **2001**, *37*, 859−861.
(19) Syms, R.; Gormley, C.; Blackstone, S. *Sens. Actuators, A* **2001**, *88*, 273−283.
(20) Bordel, D.; Putaux, J. L.; Heux, L. *Langmuir* **2006**, *22*, 4899−4901.
(21) Habibi, Y.; Heim, T.; Douillard, R. *J. Polym. Sci., Part B: Polym. Phys.* **2008**, *46*, 1430−1436.
(22) Hoeger, I.; Rojas, O. J.; Efimenko, K.; Velev, O. D.; Kelley, S. S. *Soft Matter* **2011**, *7*, 1957−1967.
(23) Kim, J.; Chen, Y.; Kang, K. S.; Park, Y. B.; Schwartz, M. *J. Appl. Phys.* **2008**, *104*, 096104−096104.
(24) Kvien, I.; Oksman, K. *Appl. Phys. A: Mater. Sci. Process* **2007**, *87*, 641−643.
(25) Sano, M. B.; Rojas, A. D.; Gatenholm, P.; Davalos, R. V. *Ann. Biomed. Eng.* **2010**, *38*, 2475−2484.
(26) Csoka, L.; Hoeger, I. C.; Peralta, P.; Peszlen, I.; Rojas, O. J. *Colloid Interface Sci.* **2011**, *363*, 206−212.
(27) Mashkour, M.; Tajvidi, M.; Kimura, T.; Kimura, F.; Ebrahimi, G. *BioResources* **2011**, *6*, 4731−4738.
(28) Sundar, S. T.; Sain, M. M.; Oksman, K. *Carbohydr. Polym.* **2010**, *80*, 35−43.
(29) Savitz, D. A.; Loomis, D. P. *Am. J. Epidemiol.* **1995**, *141*, 123−134.
(30) Rosen, A. D. *Cell Biochem. Biophys.* **2003**, *39*, 163−173.
(31) Yunker, P. J.; Still, T.; Lohr, M. A.; Yodh, A. *Nature* **2011**, *476*, 308−311.
(32) Uetani, K.; Yano, H. *Soft Matter* **2013**, *9*, 3396−3401.
(33) Nishida, R.; Takahashi, M. *Polym. J.* **2007**, *40*, 148−153.
(34) Halliday, D.; Resnick, R.; Walker, J. *Fundamentals of Physics Extended*, 10th ed.; Wiley: New York, 2013; p 278.